2.5.1.3. *Resolution*

The momentum resolution in energy-dispersive diffraction is limited by the angular divergence of the incident and diffracted X-ray beams and by the energy resolution of the detector system. The observed profile is a convolution of the profile due to the angular divergence and the profile due to the detector response. For resolution calculations, it is usually assumed that the profiles are Gaussian, although the real profiles might exhibit geometrical and physical aberrations (Subsection 2.5.1.5). The relative full width at half-maximum (FWHM) of a diffraction peak in terms of energy is then given by

$$\delta E/E = [(e_n/E)^2 + 5.546F\varepsilon/E + (\cot\theta_0\Delta\theta_0)^2]^{1/2}, \quad (2.5.1.2)$$

where e_n is the electronic noise contribution, F the Fano factor, ε the energy required for creating an electron–hole pair (*cf.* Subsection 7.1.5.1), and $\Delta\theta_0$ the overall angular divergence of the X-ray beam, resulting from a convolution of the incident- and the diffracted-beam profiles. For synchrotron radiation, $\Delta\theta_0$ can usually be replaced by the divergence of the diffracted beam because of the small divergence of the incident beam.

Fig. 2.5.1.3 shows $\delta E/E$ as a function of Bragg angle θ_0. The curves have been calculated from equations (2.5.1.1) and (2.5.1.2) for two values of the lattice-plane spacing and two values of $\Delta\theta_0$, typical for *Bremsstrahlung* and synchrotron radiation, respectively. It is seen that in all cases $\delta E/E$ decreases with decreasing angle (*i.e.* increasing energy) to a certain minimum and then increases rapidly. It is also seen that the minimum point of the $\delta E/E$ curve is lower for the small d value and shifts towards smaller θ_0 values for decreasing $\Delta\theta_0$. Calculations of this kind are valuable for optimizing the Bragg angle for a given sample and other experimental conditions (*cf.* Fukamachi, Hosoya & Terasaki, 1973; Buras, Niimura & Olsen, 1978).

The relative peak width at half-height is typically less than 1% for energies above 30 keV. When the observed peaks can be fitted with Gaussian functions, one can determine the centroids of the profiles by a factor of 10–100 better than the $\delta E/E$ value of equation (2.5.1.2) would indicate. Thus, it should be possible to achieve a relative resolution of about 10^{-4} for high energies. A resolution of this order is required for example in residual-stress measurements.

The detector broadening can be eliminated using a technique where the diffraction data are obtained by means of a scanning crystal monochromator and an energy-sensitive detector (Bourdillon, Glazer, Hidaka & Bordas, 1978; Parrish & Hart, 1987). A low-resolution detector is sufficient because its function (besides recording) is just to discriminate the monochromator harmonics. The Bragg reflections are not measured simultaneously as in standard XED. The monochromator-scan method can be useful when both a fixed scattering angle (*e.g.* for samples in special environments) and a high resolution are required.

2.5.1.4. *Integrated intensity for powder sample*

The kinematical theory of diffraction and a non-absorbing crystal with a 'frozen' lattice are assumed. Corrections for thermal vibrations, absorption, extinction, *etc.* are discussed in Subsection 2.5.1.5. The total diffracted power, $P_{\mathbf{h}}$, for a Bragg reflection of a powder sample can then be written (Buras & Gerward, 1975; Kalman, 1979)

$$P_{\mathbf{h}} = hcr_e^2 VN_c^2[i_0(E)jd^2|F|^2]_{\mathbf{h}} C_p(E,\theta_0)\cos\theta_0\Delta\theta_0, \quad (2.5.1.3)$$

where $\mathbf{h}$ is the diffraction vector, r_e the classical electron radius, $i_0(E)$ the intensity per unit energy range of the incident beam evaluated at the energy of the diffraction peak, V the irradiated sample volume, N_c the number of unit cells per unit volume, j the multiplicity factor, F the structure factor, and $C_p(E,\theta_0)$ the polarization factor. The latter is given by

$$C_p(E,\theta_0) = \tfrac{1}{2}[1 + \cos^2 2\theta_0 - P(E)\sin^2 2\theta_0], \quad (2.5.1.4)$$

where $P(E)$ is the degree of polarization of the incident beam. The definition of $P(E)$ is

$$P(E) = \frac{i_{0,p}(E) - i_{0,n}(E)}{i_0(E)}, \quad (2.5.1.5)$$

where $i_{0,p}(E)$ and $i_{0,n}(E)$ are the parallel and normal components of $i_0(E)$ with respect to the plane defined by the incident- and diffracted-beam directions.

Generally, $C_p(E,\theta_0)$ has to be calculated from equations (2.5.1.4) and (2.5.1.5). However, the following special cases are sometimes of interest:

$$P = 0: \quad C_p(\theta_0) = \tfrac{1}{2}(1 + \cos^2 2\theta_0) \quad (2.5.1.6a)$$

$$P = 1: \quad C_p(\theta_0) = \cos^2 2\theta_0 \quad (2.5.1.6b)$$

$$P = -1: \quad C_p = 1. \quad (2.5.1.6c)$$

Equation (2.5.1.6*a*) can often be used in connection with *Bremsstrahlung* from an X-ray tube. The primary X-ray beam can be treated as unpolarized for all photon energies when there is an angle of 45° between the plane defined by the primary and the diffraced beams and the plane defined by the primary beam and the electron beam of the X-ray tube. In standard configurations, the corresponding angle is 0° or 90° and equation (2.5.1.6*a*) is generally not correct. However, for $2\theta_0 < 20°$ it is correct to within 2.5% for all photon energies (Olsen, Buras, Jensen, Alstrup, Gerward & Selsmark, 1978).

Equations (2.5.1.6*b*) and (2.5.1.6*c*) are generally acceptable approximations for synchrotron radiation. Equation (2.5.1.6*b*) is used when the scattering plane is horizontal and (2.5.1.6*c*) when the scattering plane is vertical.

The diffraction directions appear as generatrices of a circular cone of semi-apex angle $2\theta_0$ about the direction of incidence. Equation (2.5.1.3) represents the total power associated with this

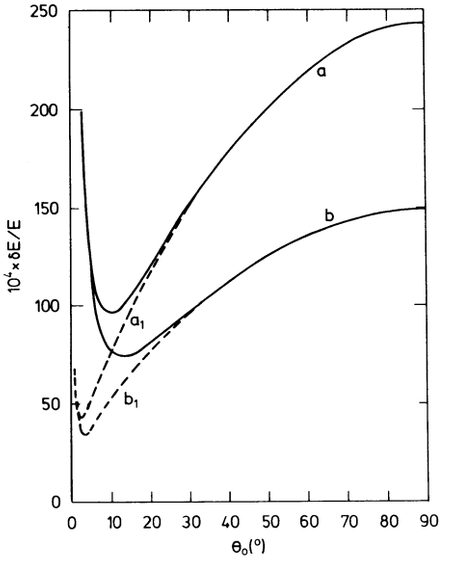

Fig. 2.5.1.3.Relative resolution, $\delta E/E$, as function of Bragg angle, θ_0, for two values of the lattice plane spacing: (*a*) 1 Å and (*b*) 0.5 Å. The full curves have been calculated for $\Delta\theta_0 = 10^{-3}$, the broken curves for $\Delta\theta_0 = 10^{-4}$.

cone. Generally, only a small fraction of this power is recorded by the detector. Thus, the useful quantity is the power per unit length of the diffraction circle on the receiving surface, $P'_{\mathbf{h}}$. At a distance r from the sample, the circumference of the diffraction circle is $2\pi r \sin 2\theta_0$ and one has (constants omitted)

$$P'_{\mathbf{h}} \propto r^{-1} V N_c^2 [i_0(E) j d^2 |F|^2]_{\mathbf{h}} \frac{C_p(E, \theta_0) \Delta\theta_0}{\sin \theta_0}. \qquad (2.5.1.7)$$

The peak areas in an XED powder spectrum are directly proportional to the $P'_{\mathbf{h}}$ of equation (2.5.1.7).

Quantitative structural analysis requires the knowledge of $i_0(E)$ and $P(E)$. As mentioned above, these quantities are not known with sufficient accuracy for *Bremsstrahlung*. For synchrotron radiation they can be calculated, but they will nevertheless contribute to the total uncertainty in the analysis. Accordingly, XED is used rather for identification of a known or assumed structure than for a full structure determination.

2.5.1.5. *Corrections*

(*a*) *Temperature effects*

The effect of thermal vibrations on the integrated intensities is expressed by the Debye–Waller factor in the same way as for standard angle-dispersive methods. Notice that $(\sin\theta)/\lambda = 1/2d$ irrespective of the method used. The contribution of the thermal diffuse scattering to the measured integrated intensities can be calculated if the elastic constants of the sample are known (Uno & Ishigaki 1975).

(*b*) *Absorption*

The transmission factor $A(E, \theta_0)$ for a small sample bathed in the incident beam and the factor $A_c(E, \theta_0)$ for a large sample intercepting the entire incident beam are the same as for monochromatic methods (Table 6.3.3.1). However, when they are applied to energy-dispersive techniques, one has to note that the absorption corrections are strongly varying with energy. In the special case of a symmetrical reflection where the incident and diffracted beams each make angles θ_0 with the face of a thick sample (powder or imperfect crystal), one has

$$A_c(E) = \frac{1}{2\mu(E)}, \qquad (2.5.1.8)$$

where $\mu(E)$ is the linear attentuation coefficient evaluated at the energy associated with the Bragg reflection.

(*c*) *Extinction and dispersion*

Extinction and dispersion corrections are applied in the same way as for angle-dispersive monochromatic methods. However, in XED, the energy dependence of the corrections has to be taken into account.

(*d*) *Geometrical aberrations*

These are distortions and displacements of the line profile by features of the geometry of the apparatus. Axial aberrations as well as equatorial divergence contribute to the angular range $\Delta\theta_0$ of the Bragg reflections. There is a predominance of positive contributions to $\Delta\theta_0$, so that the diffraction maxima are slightly displaced to the low-energy side, and show more tailing on the low-energy side than the high-energy side (Wilson, 1973).

(*e*) *Physical aberrations*

Displacements due to the energy-dependent absorption and reflectivity of the sample tend to cancel each other if the incident intensity, $i_0(E)$, can be assumed to be constant within the energy range of Bragg reflection. With synchrotron radiation, $i_0(E)$ varies rapidly with energy and its influence on the peak positions should be checked. Also, the detector response function will influence the line profile. Low-energy line shapes are particularly sensitive to the deadlayer absorption, which may cause tailing on the low-energy side of the peak. Integrated intensities, measured as peak areas in the diffraction spectrum, have to be corrected for detector efficiency and intensity losses due to escape peaks.

2.5.1.6. *The Rietveld method*

The Rietveld method (see Chapter 8.6) for refining structural variables has only recently been applied to energy-dispersive powder data. The ability to analyse diffraction patterns with overlapping Bragg peaks is particularly important for a low-resolution technique, such as XED (Glazer, Hidaka & Bordas, 1978; Buras, Gerward, Glazer, Hidaka & Olsen, 1979; Neuling & Holzapfel, 1992). In this section, it is assumed that the diffraction peaks are Gaussian in energy. It then follows from equation (2.5.1.7) that the measured profile y_i of the reflection k at energy E_i corresponding to the ith channel of the multichannel analyser can be written

$$y_i = \frac{c'}{H_k} i_0(E_i) A(E_i) j_k d_k^2 |F_k|^2 \exp\{-4 \ln 2[(E_k - E_i)^2 / H_k^2]\}, \qquad (2.5.1.9)$$

where c' is a constant, $i_0(E_i)$ is evaluated at the energy E_i, and H_k is the full width (in energy) at half-maximum of the diffraction peak. $A(E_i)$ is a factor that accounts for the absorption in the sample and elsewhere in the beam path. The number of overlapping peaks can be determined on the basis of their position and half-width. The full width at half-maximum can be expressed as a linear function of energy:

$$H_k = UE_k + V, \qquad (2.5.1.10)$$

where U and V are the half-width parameters.

2.5.1.7. *Single-crystal diffraction*

Energy-dispersive diffraction is mainly used for powdered crystals. However, it can also be applied to single-crystal diffraction.

A two-circle system for single-crystal diffraction in a diamond-anvil high-pressure cell with a polychromatic, synchrotron X-ray beam has been devised by Mao, Jephcoat, Hemley, Finger, Zha, Hazen & Cox (1988).

Formulae for single-crystal integrated intensities are well known from the classical Laue method. Adaptations to energy-dispersive work have been made by Buras, Olsen, Gerward, Selsmark & Lindegaard-Andersen (1975).

2.5.1.8. *Applications*

The unique features of energy-dispersive diffraction make it a complement to rather than a substitute for monochromatic angle-dispersive diffraction. Both techniques yield quantitative structural information, although XED is seldom used for a full structure determination. Because of the fixed geometry, energy-dispersive methods are particularly suited to *in situ* studies of samples in special environments, *e.g.* at high or low temperature and/or high pressure. The study of anomalous scattering and forbidden reflections is facilitated by the possibility of shifting the diffraction peaks on the energy scale by changing the scattering angle. Other applications are studies of Debye–Waller factors, determinative mineralogy, attenuation-coefficient measurements, on-stream measurements, particle-size and -strain

references